

A dual role for poly-ADP-ribosylation in spatial memory acquisition after traumatic brain injury in mice involving NAD⁺ depletion and ribosylation of 14-3-3 γ

Margaret A. Satchell,* Xiaopeng Zhang,* Patrick M. Kochanek,*† C. Edward Dixon,‡
Larry W. Jenkins,‡ John Melick,* Csaba Szabó§ and Robert S. B. Clark*†

Departments of *Critical Care Medicine, †Pediatrics, and ‡Neurological Surgery, Safar Center for Resuscitation Research and the Brain Trauma Research Center, University of Pittsburgh, Pittsburgh, Pennsylvania, USA

§Inotek Pharmaceuticals Corporation, Beverly, Massachusetts, USA

Abstract

Poly(ADP-ribose) polymerase-1 (PARP-1) is a homeostatic enzyme that paradoxically contributes to disturbances in spatial memory acquisition after traumatic brain injury (TBI) in transgenic mice, thought to be related to depletion of its substrate nicotinamide adenine dinucleotide (NAD⁺). In this study, systemic administration of the PARP-1 inhibitor 5-iodo-6-amino-1,2-benzopyrone (INH2BP) after TBI preserved brain NAD⁺ levels and dose-dependently reduced poly-ADP-ribosylation 24 h after injury. While moderate-dose INH2BP improved spatial memory acquisition after TBI; strikingly, both injured- and sham-mice receiving high-dose INH2BP were unable to learn in the Morris-water maze. Poly-ADP-ribosylated peptides identified using a proteomics approach yielded

several proteins potentially associated with memory, including structural proteins (tubulin α and β , γ -actin, and α -internexin neuronal intermediate filament protein) and 14-3-3 γ . Nuclear poly-ADP-ribosylation of 14-3-3 γ was completely inhibited by the dose of INH2BP that produced profound memory disturbances. Thus, partial inhibition of poly-ADP-ribosylation preserves NAD⁺ and improves functional outcome after TBI, whereas more complete inhibition impairs spatial memory acquisition independent of injury, and is associated with ribosylation of 14-3-3 γ .

Keywords: 14-3-3, DNA damage, head injury, 5-iodo-6-amino-1,2-benzopyrone, nicotinamide adenine dinucleotide, poly(ADP-ribose) synthetase.

J. Neurochem. (2003) **85**, 697–708.

Poly(ADP-ribose) polymerase-1 (PARP-1; E.C.2.4.2.30) is an abundant nuclear protein that is activated by single-strand DNA breaks, produced by a variety of insults including reactive oxygen and nitrogen species, chemical agents, and UV irradiation (Dawson and Dawson 1995; Szabo 1996). Activated PARP-1 utilizes nicotinamide adenine dinucleotide (NAD⁺) as a substrate for generating large branching adenosine diphosphate (ADP)-ribose polymers on various proteins including histones, topoisomerases, and PARP-1 itself (Szabo 1998). PARP-1 activation facilitates DNA repair by enabling other enzymes to locate and replace missing base pairs (Szabo *et al.* 1997; Bauer *et al.* 2000). Neuronal death and neurologic dysfunction after CNS injury appears to be mediated in part by activation of PARP-1, particularly CNS insults associated with DNA damage and energy failure such as cerebral ischemia (Eliasson *et al.* 1997; Endres *et al.* 1998a) and traumatic brain injury (TBI; Whalen *et al.* 1999; LaPlaca *et al.* 2001). While disruption of the PARP-1 gene

Received December 17, 2002; revised manuscript received January 14, 2003; accepted January 15, 2003.

Address correspondence and reprint requests to Robert S. B. Clark, Safar Center for Resuscitation Research, 3434 Fifth Avenue, Pittsburgh, PA 15260, USA. E-mail: clarkrs@ccm.upmc.edu

Abbreviations used: 2-AB, 3-aminobenzamide; ADP, adenosine diphosphate; CCI, controlled cortical impact; DMSO, dimethyl sulphoxide; DTT, dithiothreitol; Hsc54, heat shock cognate protein 54; IEF, isoelectric focusing; INH2BP, 5-iodo-6-amino-1,2-benzopyrone; IPG, immobilized pH gradient; LDH, lactate dehydrogenase; MALDI-MS, matrix-assisted laser desorption ionization-mass spectrometry; MTT, 3-(4,5-dimethylthiazal-2-yl)-2,5-diphenyltetrazolium bromide; NAD⁺, nicotinamide adenine dinucleotide; NIF, neuronal intermediate filament; NO, nitric oxide; PANT, polymerase I-mediated dATP nick-translation; PARP-1, poly(ADP-ribose) polymerase-1; PBS, phosphate-buffered saline; PMS, phenazine methosulfate; PMSF, phenylmethylsulphonyl fluoride; PVDF, polyvinylidene difluoride; ROD, relative optical density; SDS, sodium dodecyl sulfate; TBI, traumatic brain injury.

has been shown to be exclusively protective after acute brain injury, a recent study suggests that pharmacologic PARP-1 inhibition after brain injury may not be uniformly beneficial possibly related to impairment of DNA repair (Nagayama *et al.* 2000). Furthermore, poly-ADP-ribosylation has been shown to be important in several other homeostatic cellular functions, including transcriptional regulation (Hassa and Hottiger 1999; Kameoka *et al.* 2000; Mendoza-Alvarez and Alvarez-Gonzalez 2001; Tong *et al.* 2001; Ziegler and Oei 2001; Ha *et al.* 2002), mitosis (Smith *et al.* 1998), and long-term potentiation in neurons (Schuman *et al.* 1994; Klempisch *et al.* 1999).

A variety of PARP-1 inhibitors have been used in the study of neuronal injury. Nicotinamide and 3-aminobenzamide (3-AB) have been the most commonly used PARP-1 inhibitors; however, they are relatively non-specific and lack potency (Yoshihara *et al.* 1994; Endres *et al.* 1997). Recently, more potent and specific PARP-1 inhibitors, including 5-iodo-6-amino-1,2-benzopyrone (INH2BP), have been reported to be beneficial after temporary focal ischemia in mice (Takahashi *et al.* 1997; Endres *et al.* 1998a; Abdelkarim *et al.* 2001), and to reduce contusion area after TBI in rats (LaPlaca *et al.* 2001). None of these studies have evaluated the effect of pharmacologic PARP-1 inhibition on long-term functional or histologic outcome after injury, relevant as poly-ADP-ribosylation serves multiple homeostatic functions in addition to maintenance of genomic integrity (Szabo 1996; mentioned above).

Accordingly, we first sought to establish that PARP-1 is activated after TBI using a controlled cortical impact (CCI) model in mice. Because DNA damage produced by free radicals is felt to be the principal trigger of PARP-1, evidence for oxidative and nitrosative stress in injured brain was verified by the detection of single-strand DNA breaks and protein nitration. PARP-1 activity was assessed by examining for poly-ADP-ribosylation and depletion of NAD⁺. To determine the role of PARP-1 in neurologic recovery after TBI, the effect of the PARP-1 inhibitor INH2BP on poly-ADP-ribosylation and long-term functional and histopathologic outcome were evaluated. The specificity of the PARP-1 inhibitor was verified by treating uninjured PARP-1^{-/-} and PARP-1^{+/+} mice with INH2BP, then assessing spatial memory acquisition using the Morris-water maze. The mechanism(s) underlying the novel role for poly-ADP-ribosylation in memory formation *in vivo* was examined by using a proteomics approach to identify candidate poly-ADP-ribosylated proteins within brain.

Materials and methods

Mice

All experiments were approved by the University of Pittsburgh Institutional Animal Care and Use Committee and complied with

the NIH guide for the Care and Use of Laboratory Animals. Male C57BL/6 J mice at 12–13 weeks of age (25–35 g) and were given free access to food and water and housed in laminar flow racks in a temperature-controlled room with 12-h light–dark cycles. Homozygous male PARP-1^{-/-} and PARP-1^{+/+} littermate controls of C57BL/6 lineage were generated as previously described (Wang *et al.* 1995), bred in an animal facility, and used at 13 weeks of age (28–35 g). PARP-1^{-/-} mice were produced by deletion of part of the second exon and intron by standard techniques of homologous recombination in embryonic stem cells and the mice were genotyped as described (Wang *et al.* 1995).

Study design

Protocol 1: PARP-1 activation after TBI

Male C57BL/6 J mice underwent CCI and the brains were harvested at 8 h, 24 h, 72 h, 7 days, and 21 days. Naive mice were used as controls. Nitrosative and oxidative stress after CCI was determined indirectly by detection of nitrotyrosine residues on proteins by western blot analysis ($n = 2–3$ /group) and single-strand DNA breaks using DNA polymerase I-mediated dATP nick-translation (PANT; $n = 4$ /group at 24 h only). PARP-1 activity was determined by measuring poly-ADP-ribosylation ($n = 2–3$ /group).

Protocol 2: biochemical analysis of PARP-1 inhibition 24 h after TBI

Male C57BL/6 J mice were randomized to receive 30 or 60 mg/kg INH2BP or vehicle [dimethyl sulphoxide (DMSO)] via a single intraperitoneal (i.p.) injection immediately after either CCI or sham operation. Sham-operated controls were anesthetized and underwent craniectomy without CCI. At 24 h, mice were anesthetized with 4% isoflurane, perfused with ice-cold saline, and the brains were harvested for biochemical evaluation – poly-ADP-ribosylation and NAD⁺ quantification by enzyme cycling method.

Protocol 3: effect of PARP inhibition on functional and histological outcome after TBI

Mice were randomized to receive DMSO vehicle, 30 or 60 mg/kg INH2BP i.p., one dose at the time of injury and a second dose at 24 h. Neurological function was assessed using beam balance, round tube balance and wire grip tests for motor function on days 1–5, and the Morris-water maze to assess spatial memory acquisition on days 14–20. Mice that failed pre-testing prior to injury, defined as a wire grip score = 0 (did not stay on the wire for 30 s), were not used for assessment of functional outcome. In total, six to 10 mice/CCI group and five to six mice/sham group were used for assessment of functional outcome. At 21 days, mice were anesthetized with 4% isoflurane, perfused with 4% paraformaldehyde, and the brains processed for assessment of lesion volume and hippocampal cell counts as previously described.

Protocol 4: effect of INH2BP in uninjured PARP-1^{-/-} and PARP-1^{+/+} mice

PARP-1^{-/-} mice ($n = 10$) and PARP-1^{+/+} ($n = 5$) littermates underwent sham operation (no CCI) and were treated with INH2BP at a dose of 60 mg i.p. at the time of surgery and at 24 h. Neurological function was assessed as in protocol 3. Because a drug effect independent of injury on spatial memory acquisition was

clearly demonstrated with 60 mg/kg (protocol 3), and this dose led to complete preservation of brain NAD⁺ levels at 24 h (protocol 2), only the 60 mg/kg dose was tested in the PARP knockout mice.

Mouse cerebral trauma model

The CCI model for mice was used as previously described (Sinz *et al.* 1999; Whalen *et al.* 1999). Mice were anesthetized with 2% isoflurane (Anaquest, Memphis, TN, USA), N₂O and O₂ 2 : 1 using a nose cone. The mouse was positioned in a stereotaxic frame and a brain temperature probe (0.009 inches, Physitemp Corp, Clifton, NJ, USA) was inserted into the left frontal cortex through a burr hole. A bone flap was made on the parietal cortex using a dental drill, and mice were subjected to CCI using a pneumatic cylinder with a 5-cm stroke using a vertically driven 3-mm metal tip at a velocity of 6 m/s and a depth of penetration of 1.2 mm. After injury, the bone flap was replaced and the scalp incision was sutured. This level of injury results in reproducible motor and cognitive deficits quantified during the first and third week after injury, respectively. INH2BP or DMSO vehicle were injected i.p. at the time of injury. An additional dose was given at 24 h for long-term outcome studies (protocols 3 and 4).

Western blot analysis

The ipsilateral parietal cortex including injury site and dorsal hippocampus were homogenized in lysis buffer containing 20 mM HEPES (pH 7.8), 10 mM NaCl, 1.5 mM MgCl₂, 1 mM EDTA, 1 mM EGTA, 1 mM dithiothreitol (DTT), 1 mM phenylmethylsulfonyl fluoride (PMSF), and 2 µg/mL aprotinin. Aliquots were incubated at 4°C for 30 min and centrifuged at 16 000 g and supernatants were boiled in standard loading buffer for 5 min. Fifty-microgram protein samples, as determined by absorbance at A280 were loaded on sodium dodecyl sulfate (SDS)–polyacrylamide gels, separated electrophoretically, and transferred to a polyvinylidene difluoride (PVDF) membrane (Amersham, Arlington Heights, IL, USA) overnight. The transferred membranes were incubated in the monoclonal primary antibody against nitrotyrosine (1 : 500; clone 1A6, Upstate Biotechnology, Lake Placid, NY, USA) or poly(ADP-ribose) polymers (1 : 1000; SA-216, Biomol, Plymouth Meeting, PA, USA) at room temperature for 1 h, washed in phosphate-buffered saline (PBS) containing 0.1% Tween-20, then incubated in the appropriate secondary antibody (1 : 3000) for 1 h. The membranes were washed in PBS containing 0.1% Tween-20 three times over 60 min, then incubated in commercial enhanced chemiluminescence reagents (NEN Life Science Products, Boston, MA, USA) and exposed to X-ray film. Autoradiogram signals were semiquantified using a gel densitometric scanning program (MCID, St Catherines, Ontario, Canada).

PANT assay

PANT was performed as previously described (Clark *et al.* 2001). Briefly, paraffin-embedded 5-µm coronal sections were deparaffinized then incubated in 3% Triton X-100 (Sigma, St Louis, MO, USA) at room temperature for 1 h, then placed in 3% H₂O₂ and 30% methanol in PBS for 20 min. Sections were incubated in 40 U/mL DNA polymerase I and 29 µmol/mL biotin-14-dATP (both from Life Technologies, Gaithersburg, MD, USA) in 1 mL 1 × PANT buffer (5 mM MgCl₂, 50 mM KHPO₄, 10 mM 2-mercaptoethanol, and 30 µM each dGTP, dCTP, and dTTP) at 37°C for 90 min, washed with PBS three times, incubated in avidin–biotin complex (ABC standard kit,

Vector Laboratories, Burlingame, CA, USA), and DNA strand breaks visualized with diaminobenzidine (Vector Laboratories).

Determination of NAD⁺ levels

Tissue NAD⁺ levels were measured *ex vivo* by an enzymatic cycling method using alcohol dehydrogenase (Nisselbaum and Green 1969) with modifications. Briefly, a 3-mm slice of brain was removed and divided into ipsi- and contralateral sections. These sections were further divided superior-inferiorly, and NAD⁺ levels were determined in the superior portion, which comprised the dorsal hippocampus and the overlying cortex including the contusion. These fresh tissue samples were homogenized immediately in KPO₄ buffer (0.05 M KPhos, 0.1 M nicotinamide, pH 6.0), frozen rapidly, placed in a boiling water bath for 5 min, then cooled in an ice bath for 5 min. Samples were centrifuged for 10 min at 82 g at 4°C. The supernatants are stored at –70°C for batch analysis. Thawed samples were added to a reaction mixture containing glycyglycine buffer (0.065 M glycyglycine, 0.1 M nicotinamide, 0.5 M ethanol, pH 7.4), alcohol dehydrogenase, thiazolyl blue [3-(4,5-dimethylthiazal-2-yl)-2,5-diphenyltetrazolium bromide (MTT)] and phenazine methosulfate (PMS). NAD⁺ in the tissue sample generates NADH which reduces MTT through the intermediation of PMS to the purple formazan. The reaction was allowed to run for 5 min and the absorbance determined at A556. A standard curve was generated using known concentrations of NAD⁺, and NAD⁺ levels in the samples were calculated as µM/mg wet weight and expressed as percentage injured/contralateral hemisphere.

Evaluation of motor function

Motor function was assessed at 1–5 days after injury using beam balance, round tube balance, and wire grip tests for mice as previously described (Sinz *et al.* 1999; Whalen *et al.* 1999) by observers unaware of experimental group. Each day, three trials were performed for each test and the duration that the mice remained on the beams or wire was recorded, with the latency defined as the average of the three trials. The maximum latency before the mice were removed from the apparatus was 60 s for beam balance and 30 s for wire grip tests. A wire grip score was also recorded, defined as: 0 = fell off wire within the 30-s period, 1 = held on in some way for 30 s, 2 = held on with four paws for ≥ 5 s, 3 = held on with four paws and placed tail on wire for ≥ 5 s, 4 = held on with four paws, placed tail on wire and traveled along wire for ≥ 5 s, traveled to one of the vertical points within the 30-s test period. Baseline assessment (pre-testing) was done the day before injury. Mice that failed pre-testing prior to injury, defined as a wire grip score = 0, were not used for assessment of functional outcome.

Assessment of spatial memory acquisition

Spatial memory acquisition was assessed using the Morris-water maze for mice as previously described (Sinz *et al.* 1999; Whalen *et al.* 1999) by observers unaware of experimental group. Briefly, a white pool (83-cm diameter, 60-cm deep) filled with 24°C water to 29-cm depth was situated in a room with several extra maze cues located on the walls. Contained within the pool was a 10-cm round goal platform, located 1-cm below the surface of the water approximately 15-cm from the southwest wall. A video tracking system mounted above the pool (Chromotrack 3.0, San Diego Instruments, San Diego, CA, USA) recorded the swimming

movements of the mice. To ensure recovery from motor deficits, testing was performed on days 14–20 after CCI. Each mouse was subjected to a series of four trials/day. For each trial, mice were randomized to one of four starting locations and placed in the pool. Mice were given a maximum of 120 s to find the submerged platform. Mice were placed in a 37°C incubator for 4 min between trials. Performance in the Morris-water maze was quantified by the latency to find the platform. To exclude differences, motor performance between groups during Morris-water maze testing, swim speeds were determined for each mouse on day 19.

Probe trials were also conducted on days 19 and 20. After removing the platform from the Morris-water maze, mice were placed in the northwest quadrant of the maze. The video tracking system was used to record swim speeds and time within each quadrant over a 60-s period. The percentage time spent in the target (southwest) quadrant was determined for each animal.

Histologic analysis

Morphometric image analysis (MCID Imaging Systems) was used to determine contusion, ventricular, and hemispheric volumes at 21 days after CCI by an observer blinded to experimental group. Coronal sections (20- μ m) were cut at 0.5-mm distances from the anterior to the posterior brain and mounted on glass slides. At each 0.5-mm interval, four sections were obtained and stained with cresyl violet. The areas of the lesion, left lateral ventricle, and injured and non-injured hemispheres from each section were determined. From these data, lesion, ventricular, and hemispheric volumes were calculated. Surviving neurons in the CA1 and CA3 hippocampal regions from the dorsal hippocampus directly below the impact were counted for each mouse at 400 \times by an observer blinded to treatment group.

Immunoprecipitation, two-dimensional gel electrophoresis and MALDI-MS

Separate mice subjected to CCI were treated with either 30 or 60 mg of INH2BP or vehicle *i.p.* as described above ($n = 4$ –5/group). An additional four naive mice were used as control. At 24 h, brains were removed and proteins extracted as described above. For immunoprecipitation, 200 μ g of pooled whole-cell lysates were placed in 500 μ L cold lysis buffer (0.1 M NaCl, 0.01 M Tris, 0.1 mM EDTA, with protease inhibitors). Samples were mixed with 20 μ L of mouse or rabbit IgG agarose conjugate at 4°C for 30 min with gentle agitation. Samples were centrifuged at 1000 *g* at 4°C for 5 min. Supernatants were incubated with 2 μ g antipoly(ADP-ribose) polymer (SA-216, Biomol) or rabbit polyclonal anti-rat 14-3-3 γ (C-16; Santa Cruz Biotechnology, Santa Cruz, CA, USA) antibody at 4°C for 1 h with agitation, then mixed with 20 μ L protein A/G PLUS-agarose (Santa Cruz) and incubated overnight at 4°C with agitation. Immunoprecipitates were centrifuged at 1000 *g* for 5 min at 4°C. Pellets were washed four times followed by centrifugation, then resuspended in 50 μ L protein resuspension reagent (ProteoPrep Universal Extraction Kit, Sigma). Western blot was performed as described above.

Protein two-dimensional (2D) gel electrophoresis was performed as previously described (Jenkins *et al.* 2002). Briefly, pooled protein samples ($n = 4$ –5/group) were mixed with 300 μ L immobilized pH gradient (IPG) strip rehydration buffer (7 M urea, 2 M thiourea, 0.8% CHAPS, 1% DTT, 0.8% carrier ampholytes, 1% zwittergen, and 0.01% bromophenol blue). Isoelectric focusing (IEF) for the first

dimension protein separation was performed using an IPG phaser apparatus and Investigator 5000 V 2D Power Supply (Genomic Solutions, Inc., Ann Arbor, MI, USA) and 18-cm ProteoGel IPG strips (Sigma) rehydrated overnight with the sample/rehydration buffer mixture. The strips were rehydrated in the same trays as the IEF was conducted. The strips were run the following day using a ramping IPG strip (200–5000 V) focusing algorithm for overnight IEF to obtain a final focusing voltage of 5000 V and 100 000 Vh. Following IEG, the focused IPG strips were sequentially equilibrated with IPG equilibration buffer 1 (6 M urea, 2% DTT, 30% glycerol, 2% SDS) and buffer 2 (6 M urea, 2.5% idoacetamide, 30% glycerol, 2% SDS). The strips were loaded on top of Tris–Tricine slab gels (Genomic Solutions, Inc.) which were electrophoresed for 5 h at 20 W/gel at a controlled temperature of 18°C using a Peltier chiller in running buffer (0.2 M Tris, 0.2 M tricine, 0.4% SDS). The gels were then fixed in 40% methanol/10% acetic acid at ambient temperature for 1 h and stained with 300 mL Sypro Ruby Fluorescent Stain (Genomic Solutions, Inc.) overnight, washed in 10% methanol/6% acetic acid, and visualized under UV light. Protein spots of interest were manually punched out using a 1.5-mm 2D spot picker (The Gel Company, San Francisco, CA, USA). Peptide samples were then analyzed by matrix-assisted laser desorption ionization-mass spectrometry (MALDI-MS; Protein Chemistry Core Facility, Howard Hughes Medical Institute/Columbia University, New York, NY, USA).

Statistical analysis

Data are expressed as mean \pm SEM. Biochemical data were analyzed using Kruskal–Wallis and Dunn's post-hoc tests for non-parametric data. For functional outcome, repeated measures ANOVA with Bonferroni's post-hoc tests were used to determine group effects between injured and sham groups, and either one-way ANOVA with Tukey's tests or Kruskal–Wallis with Dunnett's post-hoc tests for normally distributed or non-parametric data, respectively, were used to determine changes from baseline. Analysis was performed using SPSS or Sigma Stat software (Jandel Scientific/SPSS, Chicago, IL, USA).

Results

Initiators of PARP-1 and PARP-1 activation in injured brain

The PANT assay was used to detect single-strand DNA damage, the principal activator of PARP-1 after cell injury, in mouse brain. PANT labeled cells were not detected in sections from control brain (Fig. 1a). At 24 h after CCI, PANT-labeled cells were consistently detected in ipsilateral cortex, the granule cell layers of CA1 and CA3 hippocampus, and dentate gyrus (Fig. 1b). PANT labeling was primarily nuclear and, based on the size, morphology, and location of the stained cells, appeared to occur in neurons. Previous dual-label studies in rats have detected PANT in mostly neuronal phenotypes (Clark *et al.* 2001). PANT was not detected in the contralateral hemispheres, or in deeper brain regions after CCI.

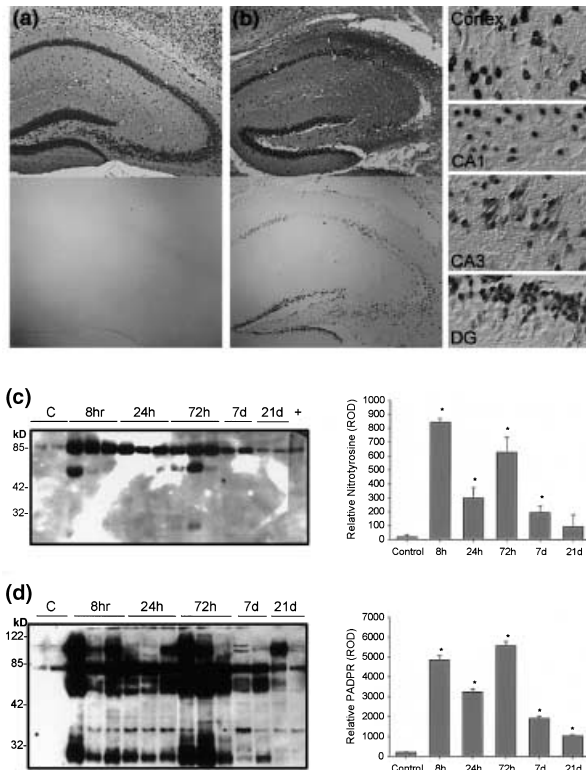


Fig. 1 Biochemical evidence of PARP-1 activation after TBI in mice. (a and b) Cresyl violet staining and PANT labeling of the dorsal hippocampus in a representative naive mouse and an injured mouse 24 h after CCI. (a) Low magnification (40 \times) showing normal cellular architecture (top panel) and absence of PANT labeling (bottom panel) in the control mouse. (b) Twenty-four hours after CCI, significant hippocampal cell loss (top panel) and PANT-labeled cells (bottom panel) can be seen throughout both hippocampus and overlying cortex. Higher magnification differential interference contrast images (400 \times) showing PANT labeling primarily in nuclei within the granular layers of the ipsilateral cortex, CA1 and CA3 hippocampus, and dentate gyrus. Representative of four mice/group. (c) Western blot showed nitrated proteins of approximately 50 kDa and approximately 80 kDa detected at 8, 24, 72 h, and 7 and 21 days in injured mice. The ROD of the nitrotyrosine residues on the approximately 50-kDa and 80-kDa proteins were increased at 8, 24, 72 h, and 7 days after injury versus naive controls (mean \pm SEM; $n = 2\text{--}3$ /group; $*p < 0.05$). (d) PARP-1 activation after injury as measured by poly-ADP-ribosylation. Poly(ADP-ribose) polymers were detected at 8, 24, 72 h and 7 and 21 days after TBI on approximately 30-, 50-, 85-, and 115-kDa protein bands. The ROD of the approximately 30-, 50-, 85-, and 115-kDa proteins was increased at all time points after CCI versus naive controls (mean \pm SEM; $n = 2\text{--}3$ /group; $*p < 0.05$).

A potent inducer of single-strand DNA breaks is peroxy-nitrite generated by the reaction of nitric oxide (NO) and superoxide. Peroxynitrite is difficult to measure *in situ*; however, a surrogate marker for peroxy-nitrite (in addition to single-strand DNA breaks) is nitration of amino acids on proteins, which can readily be detected using antibodies

against nitrotyrosine (Beckmann *et al.* 1994). Western blot analysis detected nitrotyrosine residues as early as 8 h, persisting for up to 7 days, and returning to baseline by 21 days after CCI (Fig. 1c). Minimal nitrotyrosine residues were detected in brains of control animals. Semi-quantification of relative optical densities (ROD) of this zymogram showed that nitrotyrosine residues were increased at 8, 24 and 72 h and 7 days after injury compared with control ($p < 0.05$). The predominant protein band was approximately 80 kDa, and corresponded to a nitrated albumin-positive control.

PARP-1 activation was measured indirectly by western blot detection of poly-ADP-ribosylation. Poly-ADP-ribosylation was increased at all time points after CCI compared with control ($p < 0.05$), and was maximal at 8 and 72 h (Fig. 1d). This bimodal temporal pattern was also seen with protein nitration. Minimal poly-ADP-ribosylation was detected in brains of control animals. Poly-ADP-ribosylation were predominately detected on proteins with molecular weights of approximately 115, 85, 50, and 30 kDa.

INH2BP inhibits poly-ADP-ribosylation and preserves NAD⁺ levels in injured brain

To verify that PARP activation was inhibited by INH2BP *in vivo*, the effect of INH2BP on poly-ADP-ribosylation and NAD⁺ levels were assessed 24 h after CCI. Mice treated with vehicle demonstrated a pattern of poly-ADP-ribosylation similar to untreated mice. In contrast, mice treated with INH2BP showed a dose-dependent reduction in poly-ADP-ribosylation (Figs 2a and b), with a 47% reduction after a single 30 mg/kg dose, and a 67% reduction after a single 60 mg/kg dose (both $p < 0.05$ vs. vehicle).

At 24 h, NAD⁺ levels in injured brain are typically reduced and were $57 \pm 4.3\%$ of the contralateral brain regions in the vehicle-treated group (Fig. 2c). Treatment with 60 mg/kg INH2BP preserved NAD⁺ levels in injured brain ($107 \pm 40\%$ of contralateral brain regions; $p < 0.05$ vs. vehicle). When NAD⁺ levels were examined using $\mu\text{M}/\text{mg}$ wet weight rather than percentage of contralateral brain regions, values obtained for both the 30 and 60 mg/kg treatment groups, but not the vehicle group, were similar to control (control = 1.48 ± 0.05 , vehicle = 1.10 ± 0.18 , 30 mg/kg = 1.61 ± 0.21 and 60 mg/kg = 1.56 ± 0.23 $\mu\text{M}/\text{mg}$ wet weight), consistent with the possibility that high-dose INH2BP reduces poly-ADP-ribosylation without further preservation of NAD⁺ content. These data are consistent with inhibition of PARP-1 in injured brain by systemic treatment with INH2BP.

Effect of pharmacological PARP-1 inhibition on functional and histologic outcome

Fifty-eight mice were randomized in Protocol 3. Five mice died after treatment across groups. Of the remaining mice, five failed pre-testing (wire grip score = 0 before injury),

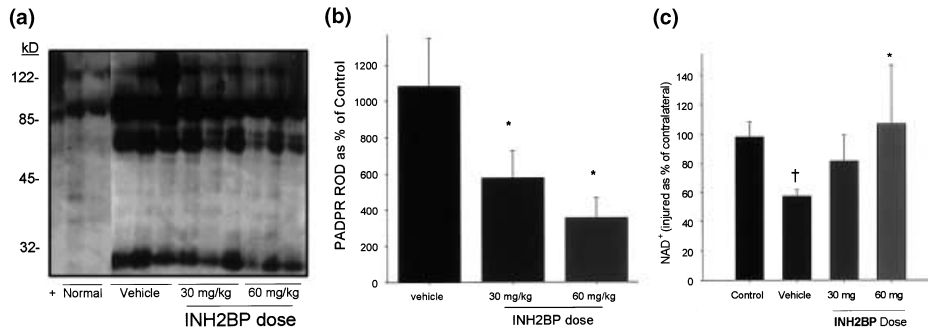


Fig. 2 INH2BP reduces PARP-1 activation in injured brain in a dose-dependent manner. (a) Western blot of injured brain tissue from animals treated with 30 or 60 mg/kg INH2BP or an equal volume of DMSO vehicle. (b) Graph of the ROD of the approximately 30-, 60-, 85-, and 115-kDa protein bands showing a dose-dependent decrease in poly-ADP-ribosylation with INH2BP treatment (mean \pm SEM; $n = 3$ /treatment group; $*p < 0.05$ vs. vehicle). (c) INH2BP preserves NAD⁺

content in injured brain tissue 24 h after CCI. NAD⁺ levels are expressed as the percentage of injured/contralateral brain samples. A decrease in NAD⁺ levels is seen after injury in vehicle-treated animals compared with uninjured controls. NAD⁺ level is preserved in animals treated with 60 mg/kg INH2BP (mean \pm SEM; $n = 5$ /group; $\dagger p < 0.05$ vs. control; $*p < 0.05$ vs. vehicle).

and therefore were excluded from functional outcome analysis. A breakdown of the sample sizes for each group for Protocol 3 is as follows: CCI + vehicle, $n = 6$; CCI + 30 mg/kg INH2BP, $n = 10$; CCI + 60 mg/kg, $n = 9$; sham + vehicle, $n = 6$; sham + 30 mg/kg INH2BP, $n = 6$; sham + 60 mg/kg, $n = 6$. Gross behavior was similar between treatments within the injured and sham groups. Over the 21-day period, a modest weight gain was seen in all CCI groups (1.4 ± 0.5 , 0.8 ± 0.6 g and 0.8 ± 0.3 g for the vehicle, 30 mg/kg and 60 mg/kg INH2BP groups, respectively; $p > 0.05$).

Spatial memory acquisition determined using the Morris-water maze apparatus is shown in Fig. 3. The sham, vehicle-treated animals demonstrate a typical pattern of decreasing latency to find the platform over the five testing days, whereas the injured, vehicle-treated mice were unable to learn in the Morris-water maze as demonstrated by the lack of improvement in latencies to find the hidden platform ($p = 0.001$, sham-vehicle vs. injured-vehicle). Sham animals given 30 mg/kg \times 2 INH2BP similarly demonstrated decreasing latency over time, though with longer latencies to find the platform initially, but an accelerated rate of recovery compared with the sham-vehicle group. Injured animals given 30 mg/kg \times 2 INH2BP demonstrated a modest, but significant, ability to learn over time ($p < 0.05$ vs. baseline). In contrast to the group treated with moderate-dose INH2BP, but similar to the vehicle-treated group, mice treated with 60 mg/kg \times 2 INH2BP were unable to learn in the Morris-water maze. Strikingly, the performance of the sham-operated and injured mice treated with 60 mg/kg \times 2 INH2BP did not differ, with both groups showing marked impairment in Morris-water maze performance. These data demonstrate a U-shaped dose-related effect of INH2BP on ability to learn in the Morris-water maze after injury. In fact, the Morris-water maze performance of the sham-60

mg/kg-treated group was significantly worse than the sham-vehicle-treated group ($p = 0.033$). With the exception of differences between the sham-vehicle and injured-vehicle groups, and the sham-vehicle- and sham-60 mg/kg-treated groups, there were no between-group differences. Results of the probe trials did not detect differences in the percentage of time spent in the target quadrant between any of the groups (data not shown). This is not surprising, as probe trial performance may not be as reliable in mice compared with rats (Frick *et al.* 2000). There were no differences in swim speeds within injured and sham subgroups, suggesting that differences in performance were not related to persistent motor function deficits (data not shown).

Motor function tests are shown in Fig. 3(d). After CCI, mice typically develop motor function deficits which can be quantified using various tests, including the traditional and round tube beam balance and wire grip apparatus. Treatment with either 30 or 60 mg/kg INH2BP i.p. at 0 and 24 h did not effect motor performance in any of these three tests. For each paradigm, latencies were measured daily, at baseline, and on days 1–5 after CCI. Data are presented as cumulative latencies measured on days 1–5; however, no differences were detected on any individual day.

Histopathologic outcome at 3 weeks after injury is shown in Table 1. No difference was seen between treatments for the CCI and sham groups. There was a trend toward an increase in surviving CA1 and CA3 hippocampal neurons in the 30 mg/kg \times 2 INH2BP-treated mice after CCI compared with vehicle-treated mice after CCI ($p = 0.09$).

Effect of INH2BP on spatial memory acquisition in PARP-1^{-/-} and PARP-1^{+/+} transgenic mice

To determine whether INH2BP was specific for PARP-1, sham PARP^{-/-} and PARP-1^{+/+} mice were treated with 60 mg/kg INH2BP i.p. at 0 and 24 h, and functional outcome

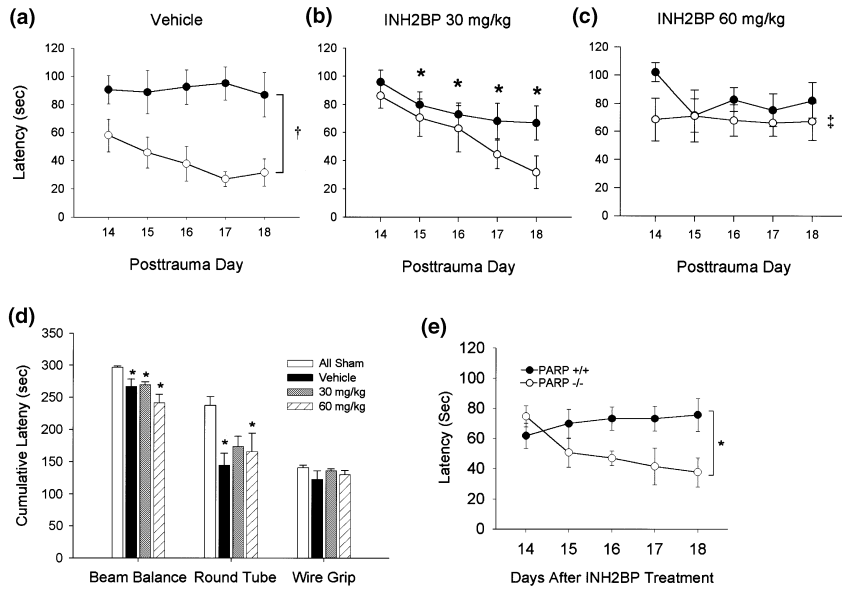


Fig. 3 Partial inhibition improves spatial memory acquisition; whereas more complete inhibition of poly-ADP-ribosylation prevents spatial memory acquisition independent of injury. (a–c) Morris-water maze performance, expressed as latency in seconds to find the submerged platform, measured on days 14–18 after CCI. ○, Sham-operated groups; ●, injured groups. (a) Injured vehicle-treated animals showed no improvement in latency to find the hidden platform over time, whereas sham-operated vehicle-treated animals showed a typical pattern of decreasing latency over time. (b) Injured animals treated with 30 mg/kg INH2BP demonstrated improved performance over the 5-day testing period ($*p < 0.05$ vs. latency on day 14 – baseline). An effect of 30 mg/kg INH2BP in sham-operated animals is suggested, when compared to the vehicle-treated sham group. (c) Animals treated with 60 mg/kg INH2BP in both injured and sham groups demonstrated no improvement in latency to find the hidden platform. Mean \pm SEM, $n = 6$ –10/group. A group difference was detected between the sham

vehicle-treated and injured vehicle-treated groups ($\dagger p = 0.001$). A group difference was also detected between the sham vehicle-treated and sham 60 mg/kg INH2BP groups, demonstrating that INH2BP at high dose impairs learning independent of injury ($\ddagger p = 0.03$). (d) Motor function performance of sham-operated and injured mice treated with INH2BP or vehicle. Individual latencies were recorded daily on days 1–5 for each task, and cumulative latencies are shown for beam balance, round tube balance, and wire grip tasks. An expected decrease in latency was seen in beam balance in all injured animals irrespective of treatment. An expected decrease in latency was seen in round tube balance in vehicle and 60 mg/kg INH2BP-treated animals. All groups performed similarly in the wire grip task. $*p < 0.05$ versus sham, mean \pm SEM, $n = 6$ –10/group. (e) Morris-water maze performance in sham-operated PARP $^{-/-}$ and PARP-1 $^{+/+}$ mice treated with 60 mg/kg INH2BP. INH2BP impaired performance in PARP $^{+/+}$ (●) but not PARP $^{-/-}$ mice (○; $p < 0.05$).

was assessed using the same paradigm used in Protocol 3. The effect of high-dose INH2BP (60 mg/kg \times 2) on Morris-water maze performance in sham PARP-1 $^{+/+}$ mice could not be demonstrated in PARP-1 $^{-/-}$ littermates (Fig. 3e). PARP-1 $^{-/-}$ mice do not have baseline learning deficits determined using the Morris-water maze (Whalen *et al.* 1999). Probe trial performance was not different between PARP-1 $^{+/+}$ and PARP-1 $^{-/-}$ mice (data not shown).

Poly-ADP-ribosylated proteins in mouse brain

A proteomics approach was used to further explore the role of poly-ADP-ribosylation in memory formation. First, brain protein homogenates were immunoprecipitated with antibody against poly(ADP-ribose) polymers to concentrate target proteins. Then, these proteins were separated using 2D gel electrophoresis (Fig. 4a) and peptide spots were identified using MALDI–MS. Eleven proteins were identified including IgG used for immunoprecipitation, which was anticipated and sent for MALDI–MS as validation of the

methods (Table 2). Twenty-seven spots were unidentified (not all are shown in Fig. 4). Of the identified proteins, many were associated with cell structure, including γ -actin, a protein similar to α internexin neuronal intermediate filament (NIF) protein, and tubulin α and β . Other ribosylated proteins included 14-3-3 γ , albumin, lactate dehydrogenase (LDH), and the chaperone proteins μ -crystallin and heat shock cognate protein 54 (Hsc54); although based on the observed molecular mass and the fact that Hsc54 represents a truncated variant of Hsc70 (Tsukahara *et al.* 2000), it is likely that this protein is Hsc70. 14-3-3 γ , μ -crystallin, α internexin NIF, LDH, and tubulin α and β were not detected in poly(ADP-ribose) polymer-immunoprecipitated samples from the contralateral hemispheres of mice treated with high-dose systemic INH2BP (Fig. 4b).

Because 14-3-3 proteins have been implicated in learning and memory (Philip *et al.* 2001), 14-3-3 γ is altered in brain tissue from patients with Alzheimer’s disease and Down’s syndrome (Fountoulakis *et al.* 1999; Peyril *et al.* 2002), and

	INH2BP dose		
	Vehicle	30 mg	60 mg
Contusion volume (mm ³)	8.9 ± 1.1	9.9 ± 1.8	9.6 ± 0.7
% Uninjured hemisphere	8.6 ± 1.0	8.7 ± 1.5	8.7 ± 0.9
Ipsilateral hippocampal volume (mm ³)	5.1 ± 0.6	6.7 ± 0.6	5.6 ± 0.6
% Uninjured hemisphere	4.8 ± 0.4	6.0 ± 0.5	4.9 ± 0.4
CA1 hippocampus			
Neuron count – ipsilateral	35 ± 11	72 ± 18	22 ± 8
Neuron count – % uninjured hemisphere	16.6 ± 4.3	34.8 ± 11.4	16.8 ± 6.8
Neuron density – ipsilateral (neurons/hpf)	26.3 ± 6.3	42.9 ± 6.3	26.0 ± 8.5
Neuron density – % uninjured hemisphere	44.3 ± 11.8	64.7 ± 11.5	60.8 ± 21.1
CA3 hippocampus			
Neuron count – ipsilateral	7 ± 3	31 ± 17	11 ± 7
Neuron count – % uninjured hemisphere	8.2 ± 3.7	28.8 ± 16.1	10.1 ± 6.2
Neuron density – ipsilateral (neurons/hpf)	7.2 ± 3.3	14.1 ± 6.1	9.7 ± 5.3
Neuron density – % uninjured hemisphere	16.4 ± 7.4	25.7 ± 11.7	19.8 ± 11.0

Mean ± SEM; hpf, high power field (400×).

Table 1 Effect of INH2BP on histologic outcome

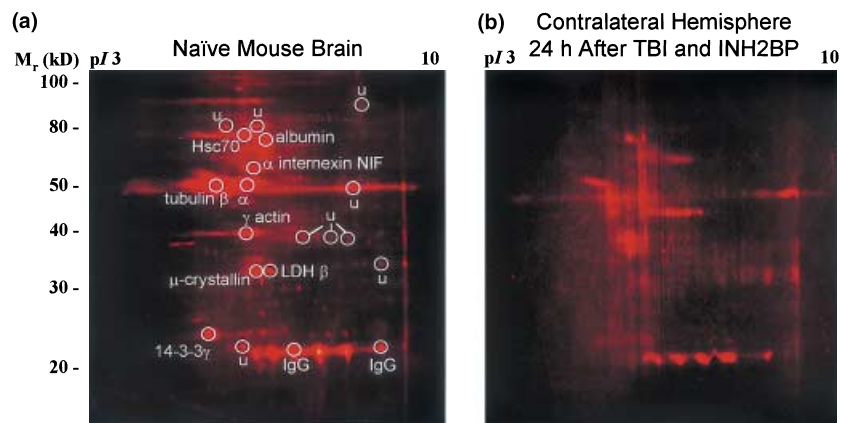


Fig. 4 Poly-ADP-ribosylated proteins in brain. Two-dimensional gel electrophoresis of proteins coprecipitated using an antibody against poly(ADP-ribose) polymers in naive mouse brain (a) and from the contralateral hemisphere of mice harvested 24 h after TBI and systemic treatment with 60 mg/kg INH2BP (b). Samples from three to four mice/group were pooled. Brain poly-ADP-ribosylated peptides from

naive mice were analyzed using MALDI-MS. Identified proteins included 14-3-3 γ , γ -actin, α internexin neuronal intermediate filament (NIF), tubulin α and β , heat shock cognate protein 70 (Hsc70), lactate dehydrogenase (LDH), μ -crystallin, and the IgG subtypes used for immunoprecipitation. Many peptides were unidentified (u), for clarity, only nine of 27 of these were labeled.

ribosylation regulates function of 14-3-3 in bacteria (Riese *et al.* 2002), further experiments were performed examining 14-3-3 γ in naive and injured mouse brain treated with INH2BP. Figure 5 shows immunoprecipitation of brain protein lysates using antibody against 14-3-3 γ followed by western blot using antibody against poly(ADP-ribose) polymers. Sypro ruby staining of all immunoprecipitated proteins shows that neither treatment with INH2BP nor TBI affect 14-3-3 γ protein binding. Several proteins with molecular weights ranging from 15 to 40 kDa co-precipitated with 14-3-3 γ antibody and were poly-ADP-ribosylated, including 14-3-3 γ itself. Larger molecular weight peptides

co-precipitated with 14-3-3 γ , but were not poly-ADP-ribosylated. Treatment with 60 mg/kg INH2BP reduced poly-ADP-ribosylation of nuclear proteins associated with 14-3-3 γ after TBI, including 14-3-3 γ (Fig. 5a). Treatment with INH2BP did not affect poly-ADP-ribosylation of cytosolic proteins (Fig. 5b); but PARP-1 is not known to reside in the cytosol.

Discussion

The present study demonstrating evidence for PARP-1 activation after CCI in mice corroborates previous studies

Table 2 Brain poly-ADP-ribosylated peptides identified by MALDI-MS

Swiss-Prot NCBIr AC number	Protein	M_r	pI
AAH08129	14-3-3 γ protein gamma subtype (mouse)	28 303	4.8
CAA31455	γ -Actin (mouse)	41 019	5.56
P07724	Albumin (mouse)	65 892	5.53
O54983	μ -Crystallin homolog (mouse)	33 523	5.44
BAB18615	Heat shock cognate protein 54 (human)*	53 518	5.62
1IGF_L	Chain L, Igg1 Fab' fragment (mouse)	24 125	5.64
AAH18383	Similar to alpha internexin neuronal intermediate filament protein (mouse)	55 383	5.35
P16125	Lactate dehydrogenase B chain (mouse)	36 441	5.7
P05213	Tubulin α -2 chain (mouse)	50 166	4.94
P04691	Tubulin β chain (mouse)	49 963	4.79

*This protein likely represents heat shock cognate protein 70 (Hsc70) based on the observed molecular mass and the fact that Hsc54 is a truncated form of Hsc70.

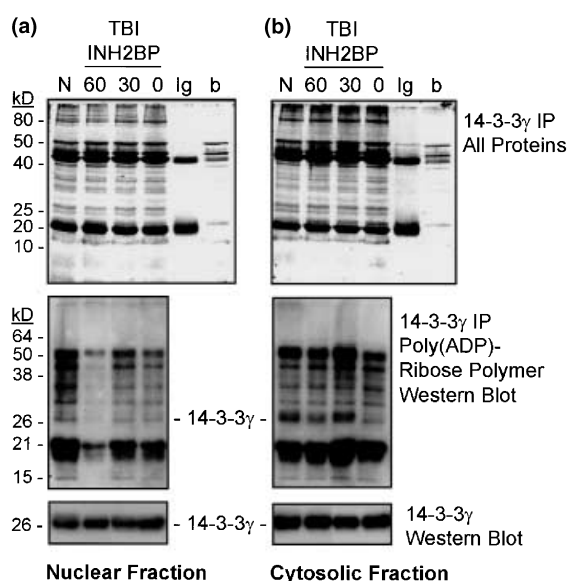


Fig. 5 INH2BP inhibits poly-ADP-ribosylation of 14-3-3 γ but does not effect 14-3-3 γ protein binding. Co-precipitation of brain homogenates from naive mice and mice 24 h after TBI treated with 30 or 60 mg/kg INH2BP i.p. or vehicle ($n = 4-5$ /group) with 14-3-3 γ . Pooled nuclear (a) and cytosolic (b) co-precipitated protein fractions were examined using Sypro Ruby staining to identify all immunoprecipitated proteins and by western blot using antibody against poly(ADP-ribose) polymers to identify poly-ADP-ribosylated proteins associated with 14-3-3 γ . Treatment with 60 mg/kg INH2BP reduced poly-ADP-ribosylation of many 14-3-3 γ -associated proteins including 14-3-3 γ itself. Treatment with INH2BP did not affect 14-3-3 γ protein binding. N, naive; Ig, co-precipitation using non-immune IgG; b, co-precipitation using only protein binding beads; IP, immunoprecipitation.

in both experimental TBI and cerebral ischemia (Eliasson *et al.* 1997; Endres *et al.* 1997; Tokime *et al.* 1998; LaPlaca *et al.* 1999). Unique to the present study, protein nitration, a surrogate marker for the presence of the potent PARP-1 activator peroxynitrite, and poly-ADP-ribosylation, a

biochemical footprint of PARP-1 activation, were evaluated for 21 days after CCI. Both were found to be persistently increased compared with normal brain, with relative peaks seen at 8 and 72 h. This temporal pattern is consistent with the bimodal elaboration of NO by constitutive followed by inducible NO synthase (iNOS) in mice, where iNOS mRNA induction is not seen until 24 h after injury (Sinz *et al.* 1999). The presence of single-strand DNA nicks, the principal trigger of PARP-1 activation, in injured brain provide further circumstantial evidence that PARP-1 is activated; although they also bring forth a potential negative impact of PARP-1 inhibition, namely inhibition of efficient DNA repair in sublethally injured brain (Nagayama *et al.* 2000). Taken together, these studies raise the possibility that biphasic cell death may also occur after TBI in this model. The first phase is partially dependent upon NAD^+ and cellular energy stores, and the second phase partially dependent upon PARP-facilitated DNA repair. We have previously shown that, in rats, caspase-3 activation peaks 24 h after TBI (Clark *et al.* 2000), and perhaps the biphasic pattern of poly-ADP-ribosylation is related to transient caspase-3 proteolytic inactivation of PARP.

A key role for PARP-1 activation after acute brain injury was established using PARP-1 knockout mice, where deletion of PARP-1 was found to confer significant protective effects in histologic and behavioral outcome (Eliasson *et al.* 1997; Endres *et al.* 1997; Whalen *et al.* 1999). Caveats related to the permanent deletion of genes exist, however, including compensatory responses and anatomical and physiologic alterations in knockout mice compared with wild-type counterparts. The therapeutic potential of pharmacologic PARP-1 inhibition has also been demonstrated in models of TBI and cerebral ischemia, although the effects have not been as robust as PARP-1 gene deletion (Endres *et al.* 1997; Takahashi *et al.* 1997; Endres *et al.* 1998b); and in a model of transient global ischemia, PARP-1 inhibition with 3-AB may have been detrimental (Nagayama *et al.*

2000). INH2BP, used in the present study, is a relatively specific and potent PARP-1 inhibitor. INH2BP inhibits PARP-1 by occupying the NAD⁺-binding site. After temporary focal ischemia in mice, a similar dose of INH2BP used in the present study (30 mg/kg × 2 i.p.) reduced infarct volumes and led to a modest improvement in neurobehavioral outcome at 72 h (Endres *et al.* 1998a). The present study shows that after TBI in mice, INH2BP inhibits PARP-1 in a dose-dependent manner and preserves brain NAD⁺ levels. Further, a modest improvement in neurobehavioral outcome (spatial memory acquisition), but not histologic outcome, was seen using moderate-dose INH2BP. Spatial memory acquisition was actually impaired in both injured and sham mice using high-dose INH2BP. These data suggest that preservation of NAD⁺ is important, but obviously not the sole determinant of recovery of spatial memory acquisition after TBI.

The finding that both injured and sham-injured mice treated with high-dose INH2BP were unable to learn in the Morris-water maze raises a question about other mechanisms of action of this PARP-1 inhibitor. Several possibilities exist as to the reason for this unexpected result. First, it is possible that high-dose INH2BP is producing undesirable systemic effects. This is refuted by the fact that there was no difference in survival, weight gain, or motor function between treatment groups. Second, complete PARP-1 inhibition may interfere with DNA repair in these animals, particularly in sublethally injured regions of brain. Nagayama *et al.* (2000) have suggested that PARP-1 activation after transient global ischemia is important for repair of single-strand DNA damage and that in the absence of NAD⁺ depletion PARP-1 activation may be neuroprotective. Thirdly, INH2BP may inhibit ADP-ribosyltransferases or proteins other than PARP-1. Potential targets include both poly- and mono ADP-ribosyl transferases such as PARP-2, a nuclear enzyme that is DNA damage-dependent but less abundant than PARP-1 (Ame *et al.* 1999), and tankyrase (Smith *et al.* 1998). Alternatively, PARP-1 may have important functions unrelated to DNA repair. Recent studies have shown that PARP-1 regulates a number of transcription factors, perhaps by either direct binding or ribosylation, including nuclear factor- κ B, AP-1, AP-2, Stat-1, SP-1, and Yin-Yang (Hassa and Hottiger 1999; Mendoza-Alvarez and Alvarez-Gonzalez 2001; Oei and Shi 2001a, 2001b; Ha *et al.* 2002); thus inhibition of PARP-1 may influence many global cellular functions. In neurons, this may manifest in the arena of memory acquisition, either through transcriptional regulation and new protein synthesis, or by ribosylation of factors important in memory formation. Ribosylation by PARP-1 may be important in NO-dependent memory formation (Kendrick *et al.* 1997), as the relatively non-selective ADP-ribosyltransferase inhibitor nicotinamide (which inhibits both mono- and poly-ADP-ribosyltransferases) suppresses long-term potentiation in hippocampal slices (Schuman *et al.*

1994; Kleppisch *et al.* 1999). Thus, based on this study and work by others, it is possible that glutamate-mediated stimulation of NO production facilitates memory formation via poly-ADP-ribosylation (Ben-Ari and Aniksztejn 1995; Pieper *et al.* 2000). Whereas the pharmacological inhibition of PARP-1 appears to be feasible and effective biochemically, the undesirable neurologic sequelae seen with complete PARP-1 inhibition should be kept in mind, and the clinical application of PARP-1 inhibitors should be approached with caution. Consistent with this notion, experimental stroke studies where dose-responses were conducted with PARP-1 inhibitors showed that, at higher doses, some or much of the neuroprotective effect was lost (Takahashi *et al.* 1997).

The finding that uninjured PARP-1^{+/+} littermates treated with high-dose INH2BP had complete deficits of spatial memory acquisition, whereas PARP-1^{-/-} mice treated with high-dose INH2BP had no such deficits, implies that INH2BP is relatively selective for PARP-1. What is not answered is the question of why PARP-1 knockout mice are able to learn at all, if complete inhibition of PARP-1 in wild-type mice produces complete deficits. It is possible or even likely that in PARP-1^{-/-} mice redundancy exists, where other mono- or poly-ADP-ribosyltransferases have adapted for PARP-1 deletion during development of the animal. The finding that basal PARP activity occurs in brain as a result of normal glutamate-NO neurotransmission, including in PARP-1-deficient mice, but to a lesser degree, supports this possibility (Pieper *et al.* 2000).

Using a proteomics approach, several biologically plausible mechanisms linking substrates of poly-ADP-ribosylation and memory have been identified in the present study. 14-3-3 γ was one such substrate. Treatment with INH2BP reduced poly-ADP-ribosylation of nuclear 14-3-3 γ , but not 14-3-3 γ protein binding. While these data suggest that ribosylation affects 14-3-3 γ function unrelated to its protein binding, it remains to be determined whether ribosylation of 14-3-3 γ affects cellular localization or degradation. 14-3-3 proteins have been implicated in learning and memory (Philip *et al.* 2001) and 14-3-3 γ is increased in brain tissue from patients with Alzheimer's disease and reduced in Down's syndrome, diseases associated with memory disturbances (Fountoulakis *et al.* 1999; Peyril *et al.* 2002). Thus, further study to delineate functional interactions between 14-3-3 γ and poly-ADP-ribosylation, for example utilizing PARP knockout mice and neuronal cultures, is warranted. Several poly-ADP-ribosylated cytoskeletal proteins were also identified, all of which have been implicated in synaptic plasticity (Kaslow *et al.* 1981; Wheal *et al.* 1998; Rao and Craig 2000; Rozental *et al.* 2001), as well as the chaperone proteins μ -crystallin and Hsc70, and LDH.

While it is apparent that PARP-1 activation in the face of energy depletion, as is typical in both TBI and cerebral ischemia, can further compromise cellular energetics through depletion of NAD⁺ it is also apparent that some degree

of PARP-1, or compensatory poly-ADP-ribosyltransferase, activity is essential for many basal cellular functions as well as memory formation. Thus, partial PARP-1 inhibition may be a more desirable approach to the treatment of brain injury than complete inhibition.

Acknowledgements

We appreciate the generous support from the National Institutes of Health/National Institute of Neurologic Diseases and Stroke RO1 NS38620 (RSBC, XZ), P50 NS30318 (RSBC, PMK, CED) and R44 NS37985 (CS); National Institutes of Health/National Institute of Child Health and Human Development T32 HD40686 (MAS), the Children's Hospital of Pittsburgh, and the Laerdal Foundation (MAS).

References

- Abdelkarim G. E., Gertz K., Harms C., Katchanov J., Dirnagl U., Szabo C. and Endres M. (2001) Protective effects of PJ34, a novel, potent inhibitor of poly(ADP-ribose) polymerase (PARP) in *in vitro* and *in vivo* models of stroke. *Int. J. Mol. Med.* **7**, 255–260.
- Ame J. C., Rolli V., Schreiber V., Niedergang C., Apiou F., Decker P., Muller S., Hoger T., Menissier-de Murcia J. and de Murcia G. (1999) PARP-2, A novel mammalian DNA damage-dependent poly(ADP-ribose) polymerase. *J. Biol. Chem.* **274**, 17860–17868.
- Bauer P. I., Buki K. G., Comstock J. A. and Kun E. (2000) Activation of topoisomerase I by poly(ADP-ribose) polymerase. *Int. J. Mol. Med.* **5**, 533–540.
- Beckmann J. S., YeY. Z., Anderson P. G., Chen J., Accavitti M. A., Tarpey M. M. and White C. R. (1994) Extensive nitration of protein tyrosines in human atherosclerosis detected by immunohistochemistry. *Biol. Chem. Hoppe Seyler* **375**, 81–88.
- Ben-Ari Y. and Aniksztejn L. (1995) A united theory for the multiple forms of LTP? *Trends Neurosci.* **18**, 519–520.
- Clark R. S. B., Kochanek P. M., Watkins S. C., Chen M., Dixon C. E., Seidberg N. A., Melick J., Loeffert J. E., Nathaniel P. D., Jin K. L. and Graham S. H. (2000) Caspase-3 mediated neuronal death after traumatic brain injury in rats. *J. Neurochem.* **74**, 740–753.
- Clark R. S. B., Chen M., Kochanek P. M., Watkins S. C., Jin K. L., Draviam R., Nathaniel P. D., Pinto R., Marion D. W. and Graham S. H. (2001) Detection of single- and double-strand DNA breaks after traumatic brain injury in rats: comparison of *in situ* labeling techniques using DNA polymerase I, the Klenow fragment of DNA polymerase I, and terminal deoxynucleotidyl transferase. *J. Neurotrauma* **18**, 675–689.
- Dawson T. M. and Dawson V. L. (1995) ADP-ribosylation as a mechanism for the action of nitric oxide in the nervous system. *New Horizons* **3**, 86–92.
- Eliasson M. J., Sampei K., Mandir A. S., Hurn P. D., Traystman R. J., Bao J., Pieper A., Wang Z. Q., Dawson T. M., Snyder S. H. and Dawson V. L. (1997) Poly(ADP-ribose) polymerase gene disruption renders mice resistant to cerebral ischemia. *Nat. Med.* **3**, 1089–1095.
- Endres M., Wang Z. Q., Namura S., Waeber C. and Moskowitz M. A. (1997) Ischemic brain injury is mediated by the activation of poly(ADP-ribose) polymerase. *J. Cereb. Blood Flow Metab.* **17**, 1143–1151.
- Endres M., Scott G. S., Salzman A. L., Kun E., Moskowitz M. A. and Szabo C. (1998a) Protective effects of 5-iodo-6-amino-1,2-benzopyrone, an inhibitor of poly(ADP-ribose) synthetase against peroxynitrite-induced glial damage and stroke development. *Eur. J. Pharmacol.* **351**, 377–382.
- Endres M., Scott G., Namura S., Salzman A. L., Huang P. L., Moskowitz M. A. and Szabo C. (1998b) Role of peroxynitrite and neuronal nitric oxide synthase in the activation of poly(ADP-ribose) synthetase in a murine model of cerebral ischemia-reperfusion. *Neurosci. Lett.* **248**, 41–44.
- Fountoulakis M., Cairns N. and Lubec G. (1999) Increased levels of 14-3-3- γ and ϵ proteins in brain of patients with Alzheimer's disease and Down's syndrome. *J. Neural. Transm. Suppl.* **57**, 323–335.
- Frick K. M., Stillner E. T. and Berger-Sweeney J. (2000) Mice are not little rats: species differences in a 1-day water maze task. *Neuroreport* **11**, 3461–3465.
- Ha H. C., Hester L. D. and Snyder S. H. (2002) Poly(ADP-ribose) polymerase-1 dependence of stress-induced transcription factors and associated gene expression in glia. *Proc. Natl Acad. Sci. USA* **99**, 3270–3275.
- Hassa P. O. and Hottiger M. O. (1999) A role of poly(ADP-ribose) polymerase in NF- κ B transcriptional activation. *Biol. Chem.* **380**, 953–959.
- Jenkins L. W., Peters G. W., Dixon C. E., Zhang X., Clark R. S., Skinner J. C., Marion D. W., Adelson P. D. and Kochanek P. M. (2002) Conventional and functional proteomics using large format two-dimensional gel electrophoresis 24 hours after controlled cortical impact in post-natal day 17 rats. *J. Neurotrauma* **19**, 715–740.
- Kameoka M., Ota K., Tetsuka T., Tanaka Y., Itaya A., Okamoto T. and Yoshihara K. (2000) Evidence for regulation of NF- κ B by poly(ADP-ribose) polymerase. *Biochem. J.* **346 Part 3**, 641–649.
- Kaslow H. R., Groppi V. E., Abood M. E. and Bourne H. R. (1981) Cholera toxin can catalyze ADP-ribosylation of cytoskeletal proteins. *J. Cell Biol.* **91**, 410–413.
- Kendrick K. M., Guevara-Guzman R., Zorrilla J., Hinton M. R., Broad K. D., Mimmack M. and Ohkura S. (1997) Formation of olfactory memories mediated by nitric oxide. *Nature* **388**, 670–674.
- Kleppisch T., Pfeifer A., Klatt P., Ruth P., Montkowski A., Fassler R. and Hofmann F. (1999) Long-term potentiation in the hippocampal CA1 region of mice lacking cGMP-dependent kinases is normal and susceptible to inhibition of nitric oxide synthase. *J. Neurosci.* **19**, 48–55.
- LaPlaca M. C., Raghupathi R., Verma A., Pieper A. A., Saatman K. E., Snyder S. H. and McIntosh T. K. (1999) Temporal patterns of poly(ADP-ribose) polymerase activation in the cortex following experimental brain injury in the rat. *J. Neurochem.* **73**, 205–213.
- LaPlaca M. C., Zhang J., Raghupathi R., Li J. H., Smith F., Bareyre F. M., Snyder S. H., Graham D. I. and McIntosh T. K. (2001) Pharmacologic inhibition of poly(ADP-ribose) polymerase is neuroprotective following traumatic brain injury in rats. *J. Neurotrauma* **18**, 369–376.
- Mendoza-Alvarez H. and Alvarez-Gonzalez R. (2001) Regulation of p53 sequence-specific DNA-binding by covalent poly(ADP-ribosylation). *J. Biol. Chem.* **276**, 36425–36430.
- Nagayama T., Simon R. P., Chen D., Henshall D. C., Pei W., Stetler R. A. and Chen J. (2000) Activation of poly(ADP-ribose) polymerase in the rat hippocampus may contribute to cellular recovery following sublethal transient global ischemia. *J. Neurochem.* **74**, 1636–1645.
- Nisselbaum J. S. and Green S. (1969) A simple ultramicro method for determination of pyridine nucleotides in tissues. *Anal. Biochem.* **27**, 212–217.
- Oei S. L. and Shi Y. (2001a) Poly(ADP-ribosylation) of transcription factor Yin-Yang 1 under conditions of DNA damage. *Biochem. Biophys. Res. Commun.* **285**, 27–31.

- Oei S. L. and Shi Y. (2001b) Transcription factor Yin-Yang 1 stimulates poly(ADP-ribosyl) ation and DNA repair. *Biochem. Biophys. Res. Commun.* **284**, 450–454.
- Peyril A., Weitzdoerfer R., Gulesserian T., Fountoulakis M. and Lubec G. (2002) Aberrant expression of signaling-related proteins 14-3-3 γ and RACK1 in fetal Down's syndrome brain (trisomy 21). *Electrophoresis* **23**, 152–157.
- Philip N., Acevedo S. F. and Skoulakis E. M. (2001) Conditional rescue of olfactory learning and memory defects in mutants of the 14-3-3 ζ gene leonardo. *J. Neurosci.* **21**, 8417–8425.
- Pieper A. A., Blackshaw S., Clements E. E., Brat D. J., Krug D. K., White A. J., Pinto-Garcia P., Favitt A., Conover J. R., Snyder S. H. and Verma A. (2000) Poly(ADP-ribosyl) ation basally activated by DNA strand breaks reflects glutamate-nitric oxide neurotransmission. *Proc. Natl Acad. Sci. USA* **97**, 1845–1850.
- Rao A. and Craig A. M. (2000) Signaling between the actin cytoskeleton and the post-synaptic density of dendritic spines. *Hippocampus* **10**, 527–541.
- Riese M. J., Goehring U. M., Ehrmantraut M. E., Moss J., Barbieri J. T., Aktories K. and Schmidt G. (2002) Auto-ADP-ribosylation of *Pseudomonas aeruginosa* ExoS. *J. Biol. Chem.* **277**, 12082–12088.
- Rozental R., Andrade-Rozental A. F., Zheng X., Urban M., Spray D. C. and Chiu F. C. (2001) Gap junction-mediated bidirectional signaling between human fetal hippocampal neurons and astrocytes. *Dev. Neurosci.* **23**, 420–431.
- Schuman E. M., Meffert M. K., Schulman H. and Madison D. V. (1994) An ADP-ribosyltransferase as a potential target for nitric oxide action in hippocampal long-term potentiation. *Proc. Natl Acad. Sci. USA* **91**, 11958–11962.
- Sinz E. H., Kochanek P. M., Dixon C. E., Clark R. S., Carcillo J. A., Schiding J. K., Chen M., Wisniewski S. R., Carlos T. M., Williams D., DeKosky S. T., Watkins S. C., Marion D. W. and Billiar T. R. (1999) Inducible nitric oxide synthase is an endogenous neuroprotectant after traumatic brain injury in rats and mice. *J. Clin. Invest.* **104**, 647–656.
- Smith S., Giriat I., Schmitt A. and de Lange T. (1998) Tankyrase, a poly(ADP-ribose) polymerase at human telomeres. *Science* **282**, 1484–1487.
- Szabo C. (1996) DNA strand breakage and activation of poly-ADP-ribosyltransferase: a cytotoxic pathway triggered by peroxynitrite. *Free Radic. Biol. Med.* **21**, 855–869.
- Szabo C. (1998) Role of poly(ADP-ribose) synthetase in inflammation. *Eur. J. Pharmacol.* **350**, 1–19.
- Szabo C., Lim L. H., Cuzzocrea S., Getting S. J., Zingarelli B., Flower R. J., Salzman A. L. and Perretti M. (1997) Inhibition of poly(ADP-ribose) synthetase attenuates neutrophil recruitment and exerts antiinflammatory effects. *J. Exp. Med.* **186**, 1041–1049.
- Takahashi K., Greenberg J. H., Jackson P., Maclin K. and Zhang J. (1997) Neuroprotective effects of inhibiting poly(ADP-ribose) synthetase on focal cerebral ischemia in rats. *J. Cereb. Blood Flow Metab.* **17**, 1137–1142.
- Tokime T., Nozaki K., Sugino T., Kikuchi H., Hashimoto N. and Ueda K. (1998) Enhanced poly(ADP-ribosyl) ation after focal ischemia in rat brain. *J. Cereb. Blood Flow Metab.* **18**, 991–997.
- Tong W. M., Hande M. P., Lansdorp P. M. and Wang Z. Q. (2001) DNA strand break-sensing molecule poly(ADP-Ribose) polymerase cooperates with p53 in telomere function, chromosome stability, and tumor suppression. *Mol. Cell Biol.* **21**, 4046–4054.
- Tsukahara F., Yoshioka T. and Muraki T. (2000) Molecular and functional characterization of Hsc54, a novel variant of human heat-shock cognate protein 70. *Mol. Pharmacol.* **58**, 1257–1263.
- Wang Z. Q., Auer B., Stingl L., Berghammer H., Haidacher D., Schweiger M. and Wagner E. F. (1995) Mice lacking ADPRT and poly(ADP-ribosyl) ation develop normally but are susceptible to skin disease. *Genes Dev.* **9**, 509–520.
- Whalen M. J., Clark R. S., Dixon C. E., Robichaud P., Marion D. W., Vagni V., Graham S. H., Virag L., Hasko G., Stachlewitz R., Szabo C. and Kochanek P. M. (1999) Reduction of cognitive and motor deficits after traumatic brain injury in mice deficient in poly(ADP-ribose) polymerase. *J. Cereb. Blood Flow Metab.* **19**, 835–842.
- Wheal H. V., Chen Y., Mitchell J., Schachner M., Maerz W., Wieland H., Van Rossum D. and Kirsch J. (1998) Molecular mechanisms that underlie structural and functional changes at the post-synaptic membrane during synaptic plasticity. *Prog. Neurobiol.* **55**, 611–640.
- Yoshihara K., Tsuyuki M., Itaya A., Tanaka Y. and Kamiya T. (1994) 3-Aminobenzamide, a potent inhibitor of poly(ADP-ribose) polymerase, causes a rapid death of HL-60 cells cultured in serum-free medium. *Mol. Cell. Biochem.* **135**, 143–151.
- Ziegler M. and Oei S. L. (2001) A cellular survival switch: poly(ADP-ribosyl) ation stimulates DNA repair and silences transcription. *Bioessays* **23**, 543–548.